Journal of Manufacturing Science and Engineering. Received September 08, 2015;
Accepted manuscript posted December 31, 2015. doi:10.1115/1.4032393

Tool deflection error of three-axis CNC milling machines, monitoring and minimizing by a virtual machining system

Mohsen Soori, first author
CAD/CAPP/CAM Research Center, Department of Mechanical Engineering, Amirkabir University of Technology (Tehran Polytechnic), 424 Hafez Avenue, Tehran 15875-4413, Iran
e-mail: mohsen.soori@gmail.com

Behrooz Arezoo, second author[1]
CAD/CAPP/CAM Research Center, Department of Mechanical Engineering, Amirkabir University of Technology (Tehran Polytechnic), 424 Hafez Avenue, Tehran 15875-4413, Iran
e-mail: barezoo@yahoo.com, arezoo@aut.ac.ir

Mohsen Habibi, third author
CAD/CAPP/CAM Research Center, Department of Mechanical Engineering, Amirkabir University of Technology (Tehran Polytechnic), 424 Hafez Avenue, Tehran 15875-4413, Iran
e-mail: mohsen.habibi.mech@gmail.com

ABSTRACT

Virtual manufacturing systems carry out the simulation of manufacturing processes in digital environment in order to increase accuracy as well as productivity in part production. There are different error sources in machine tools such as tool deflection, geometrical deviations of moving axis and thermal distortions of machine tool structures. The errors due to tool deflection is caused by cutting forces and have direct effects on dimensional accuracy and surface roughness of the parts, efficient life of the cutting tool, holder and spindle. This paper presents an application of virtual machining systems in order to improve the accuracy and productivity of part manufacturing by monitoring and minimizing the tool deflection error. The tool deflection error along machining paths are monitored to present a useful methodology in

[1] Corresponding author. Tel: +98 9121197997

controlling the produced parts with regard to desired tolerances. Suitable tool and spindle can also be selected due to ability of the error monitoring. In order to minimize the error, optimization technique based on genetic algorithms is used to determinate optimized machining parameters. Free form profile of virtual and real machined parts with tool deflection error are compared in order to validate reliability as well as accuracy of the software.

KEYWORDS: virtual machining, tool deflection error, genetic algorithm, optimization of cutting conditions

INTRODUCTION

In recent years, the complexity of industrial components have increased while their life cycle times have reduced. Also, producing accurate parts with the most efficient methods at the first trial have become the demand of modern industries. Designing, testing and optimizing manufacturing processes in virtual environments have provided a key tool to achieve these goals. Using a virtual machining system, a reduction of testing and experiments and less material waste on the shop floor can be achieved. Modeling and producing parts in a virtual environment with predicted errors have provided an effective tool in order to achieve the best accuracy of the components. Optimized process parameters can also be obtained by applying optimization methods on a simulated manufacturing process in the virtual environments. As a result, time and cost of accurate production can be decreased.

Many errors due to cutting forces, geometrical deviations of machine tool structure, thermal variations, tool wear and servo errors have an effect on the accuracy of produced parts. Static and dynamic deformations of machine tool, tool holder and cutting tool have a big portion of the total error in produced parts. The tool deflection error has direct effect on quality of produced parts as well as efficiency of part production. Dimensional accuracy and surface roughness of produced parts, number of scrap and efficient life of tool, tool holder and spindle are under influence of the tool deflection error. As a result, a virtual machining system which can monitor and minimize the error is an effective tool in order to enhance quality of produced parts as well as efficiency of part production. Also, achieving desired tolerances can be checked and suitable tools can be selected due to ability of tool deflection error monitoring, using virtual machining systems.

REVIEW OF RESEARCH WORK RELATED TO TOOL DEFLECTION ERROR

Most of the research work in this area is focused on modeling and compensation of the tool deflection error.

Lo´ pez de Lacalle et al. [1] presented a tool path selection procedure in milling of complex surfaces in order to minimize dimensional errors due to tool defection. A compensation method for surface error due to tool deflection errors of a peripheral milling operation is presented by Rao and Rao [2].

Ryu [3] considered cutting force and tool deflection error as a function of tool rotational angles and other cutting parameters to present an analytical expression. Predicted cutting forces, applied forces to cutting tool and calculated shape error due to tool deflection are considered by Dow et al. [4] in order to present a technique to compensate deflection error of small milling tools.

Simulation of the deflected cutting tool trajectory in complex surface milling is presented by Smaoui et al. [5]. To correct and compensate the tool deflection error, a trajectory simulation for deflected cutting tool is proposed. Ong and Hinds [6] presented an application of tool deflection knowledge in process planning in order to select optimal feed rates with regard to designing tolerances.

Prediction of tool deflection and tool path compensation in ball-end milling is presented by Zeroudi and Fontaine [7]. Kivanc and Budak [8] presented structural modeling of end mills in milling operations in order to predict deflection error and vibrations.

Nojedeh et al. [9] presented an enhancement in accuracy of tool paths by geometrical error compensation. An error compensation software by NC code modification is developed in order to eliminate tool path deviations created by geometrical and kinematical errors of CNC milling machine. An innovative error compensation method by modification of NC codes is introduced by Eskandari et al. [10] to compensate the volumetric errors due to positional, geometrical and thermal errors of CNC milling machine.

M. Habibi et al. [11] presented a strategy to enhance accuracy of produced parts by compensation of the tool deflection and geometrical error. Soori et al. [12] presented a virtual machining system by considering dimensional and geometrical errors of three axis CNC milling machines in order to create actual machined parts in virtual environments. Virtual machining by considering dimensional, geometrical and tool deflection error in three axis CNC milling machines is presented by Soori et al. [13].

Palanisamy et al. [14] presented a developed computer algorithm in order to optimize the cutting parameters of end milling operations by genetic algorithm. To monitor and optimize cutting process of ball end milling operations, an intelligent system using genetic algorithms is developed by Cus et al. [15]. Milfelner et al. [16] developed a condition monitoring system using genetic optimization in order to design a signal processing system as well as a detector of fault conditions in milling operations. Also, optimization of machining parameters for alumina based ceramic cutting tools by using the genetic algorithm is presented by Kumar et al. [17].

An optimization paradigm based on genetic algorithms for the determination of the cutting parameters in turning process is proposed by D'Addona and Teti [18]. Jameel et al. [19] presented a review in using the genetic algorithm to optimize the machining parameters in turning operation.

Generalized process simulation and optimization strategies by using a virtual milling system is presented by Merdol and Altintas [20] in order to predict and improve the performance of three-axis milling operations.

All of the research works on the tool deflection error presented so far have focused on modeling as well as compensating the error [1-13]. Research works [14-17] do not present a system in monitoring and minimizing the tool deflection error by using a developed virtual machining system. The other research works [18,19] are dedicated to the optimization of machining parameters in turning process. The research work [20] presents virtual cutting and optimization techniques in order to maximize the material removal rate, chip load and surface speed.

Journal of Manufacturing Science and Engineering. Received September 08, 2015;
Accepted manuscript posted December 31, 2015. doi:10.1115/1.4032393

Based on the authors' findings to date, it was determined that the area of monitoring and minimizing the tool deflection error by using a virtual machining system was insufficiently explored.

In order to minimize the tool deflection error, optimization techniques based on genetic algorithms can be used to determine the optimized machining parameters. So, efficiency of part production can be increased by minimizing unnecessary cutting forces, maximizing tool life as well as minimizing the surface roughness. Also, a system with the ability of tool deflection error monitoring can be used in the selection of suitable cutting tools as well as controlling the machined parts with regard to desired tolerances.

In the present study, tool deflection error of three-axis CNC milling machine is modeled by a virtual machining system. The aim is to provide an effective tool in virtual environments in order to improve the accuracy of produced parts and efficiency of part manufacturing by monitoring and minimizing the tool deflection error.

The tool deflection error prediction concept of 3-axis milling machine is presented in section "Tool deflection error". Cutting force modeling for flat end milling tools and optimization method by the genetic algorithm are described in sections "Modeling of cutting forces" and "Optimization by genetic algorithm" respectively. The algorithm of virtual machining software is presented in section "Virtual machining software for monitoring and minimizing the tool deflection error". Finally the experimental validation of the developed algorithms and methods are described in section "Validation".

TOOL DEFLECTION MODELS

As a result of enforcing cutting forces on the milling tool, it moves away for an amount of δ from the theoretical position of G-codes and cause errors in the machined parts. Tool deflection is an important factor in obtaining accurate surfaces and desired surface roughness in milling operations. The excessive amount of tool deflection causes failures of the cutting tool or even seriously defects of the work piece.

In order to compute the tool deflection, three are several models as below:

- A cutting force model: concentrated on the point of enforced force (the application point has to be chosen) or distributed along the cutting edge of the tool.
- A model for the deflection's calculation: a simplified model such as a cantilever beam model or a more complete one such as a finite element model.
- A geometrical model of the tool.

In the present study, the results of these different models based on calculations of cutting forces are compared and in conclusion the best model is introduced.

Kivanc and Budak [21] presented another tool deflection model which is shown as Eq. 1.

$$deflection_{\max} = c\frac{F_x}{E}\left[\frac{L1^3}{D1^4} + \frac{(L2^3 - L1^3)}{D2^4}\right]^N \quad (1)$$

Where F_x is the applied force and E is the modulus of elasticity (MPa) of the tool material. The geometrical properties of the end mill are in mm. The constant c is 9.05, 8.30 and 7.93 and constant N is 0.950, 0.965 and 0.974 for 4-flute, 3-flute and 2-flute cutters, respectively. Fig. 1 shows details of the elements in Eq. 1.

MODELING OF CUTTING FORCES

Journal of Manufacturing Science and Engineering. Received September 08, 2015;
Accepted manuscript posted December 31, 2015. doi:10.1115/1.4032393

In the present work, the cutting force model proposed by Engin and Altintas [22] is used. This model presents equations which can be parametrically defined for different helical end mills. In order to obtain cutting force equations for any type of cutting tools, values for those parameters according to tool envelop geometry should be substituted in the equations. A typical milling operation with a general end mill is shown in Fig. 2.

Where ϕ_{pj} is pitch angle of flute j, $\phi_j(z)$ is total angular rotation of flute j at level z on the XY plane, $\psi(z)$ is radial lag angle and $\kappa(z)$ is axial immersion angle. In the differential chip, dz is differential height of the chip segment, ds is the length of cutting edge and h_j is height of valid cutting edge from tool tip.

The differential tangential (dF_t), radial (dF_r) and axial (dF_a) cutting forces acting on an infinitesimal cutting edge segment are given in Eq. (2).

$$\begin{cases} dF_t = K_{te}ds + K_{tc}h(\varphi_j, k)db \\ dF_r = K_{re}ds + K_{rc}h(\varphi_j, k)db \\ dF_a = K_{ae}ds + K_{ac}h(\varphi_j, k)db \end{cases} \qquad (2)$$

Where $h(\phi_j, k)$ is the uncut chip thickness normal to the cutting edge and varies with the position of the cutting point and cutter rotation. db is the projected length of an infinitesimal cutting flute in the direction along the cutting velocity.

In flat end milling operation, the uncut chip thickness can be shown as Eq. (3) [23].

$$h(\varphi_j, k) = S_{tj} Sin(\varphi_j) \qquad (3)$$

Where S_{tj} is feed per tooth and ϕ_j is radial lag angle of tooth j can be shown as Eq. (4) [22].

$$\varphi = ndt \tag{4}$$

Where n is spindle speed (rad/s) and dt is the differential time interval for the digital integration.

In the ball end milling operation, spherical part of the tool should be considered in calculation of uncut chip thickness and can be shown as Eq. (A.1) in the appendix A [24,25].

The projected length of an infinitesimal cutting flute in the direction along the cutting velocity (db) can be shown as Eq. (5).

$$db = \frac{dz}{SinK} \tag{5}$$

Details of db and Un-cut chip thickness $h(\phi_j, k)$ are shown in Fig. 3.

The edge cutting coefficients K_{te}, K_{re} and K_{ae} are constants and related to the cutting edge length ds. The sheer force coefficients K_{tc}, K_{rc} and K_{ac} are identified either mechanistically from milling tests conducted [26,27] or by a set of orthogonal cutting tests using an oblique transformation method presented by Budak and Tekeli [28]. Sub-indices(c) and (e) represent shear and edge force components, respectively.

The cutting force coefficients, especially the edge (K_{te}, K_{re} , K_{ae})and radial (K_{rc}), increase with tool wear, hence they can be calibrated with a worn tool in order to consider the influence of wear on the process [29]. In the section "Validation", coefficients of the edge cutting as well as the sheer force are obtained by an experimental operation to validate the present research work.

Once the chip load is identified and cutting coefficients are evaluated for the local edge geometry, the cutting forces in Cartesian coordinate system can be evaluated as Eq. (6).

$$\begin{bmatrix} dF_x \\ dF_y \\ dF_Z \end{bmatrix} = \begin{bmatrix} -\sin\varphi_j \sin\kappa & -\cos\varphi_j & -\sin\varphi_j \cos\kappa \\ -\cos\varphi_j \sin\kappa & \sin\varphi_j & -\cos\varphi_j \cos\kappa \\ \cos\kappa & 0 & -\sin\kappa \end{bmatrix} \begin{bmatrix} dF_r \\ dF_t \\ dF_a \end{bmatrix} \tag{6}$$

The total cutting forces for the rotational position ϕ_j can be found by integrating as Eq. (7).

$$\begin{cases} F_x(\varphi_j) = \sum_{j=1}^{N_f} F_{xj}\left[\varphi_j(z)\right] = \sum_{j=1}^{N_f} \int_{Z_1}^{Z_2} \left[-dF_{rj} \sin\varphi_j \sin\kappa_j - dF_{tj} \cos\phi_j - dF_{aj} \sin\varphi_j \cos\kappa_j\right] dz \\ F_y(\varphi_j) = \sum_{j=1}^{N_f} F_{yj}\left[\varphi_j(z)\right] = \sum_{j=1}^{N_f} \int_{Z_1}^{Z_2} \left[-dF_{rj} \cos\varphi_j \sin\kappa_j + dF_{tj} \sin\varphi_j - dF_{aj} \cos\varphi_j \cos\kappa_j\right] dz \\ F_z(\varphi_j) = \sum_{j=1}^{N_f} F_{zj}\left[\varphi_j(z)\right] = \sum_{j=1}^{N_f} \int_{Z_1}^{Z_2} \left[dF_{rj} \cos\kappa_j - dF_{aj} \sin\kappa_j\right] dz \end{cases} \tag{7}$$

Where N_f is the number of flutes on the cutter, z_1 and z_2 are the contact boundaries of the flute which is in the cut and κ_j is axial immersion angle of flute j.

In the flat end mill the $\kappa = 90^{\circ}$, thus the cutting force of Eq. (7) can be simplified as Eq. (A.2) in the appendix A.

OPTIMIZATION BY GENETIC ALGORITHM

The genetic algorithm is an optimization technique based on natural process of evolution to solve optimization and search problems. Linear and nonlinear problems can also be solved by the algorithm. Data process in the algorithm includes a set of chromosomes or strings with an infinite length while each bit is called a gene. A population is a selected number of chromosomes and a generation is the population at a given time. Determination of six fundamental issues as chromosome representation, selection function, genetic operators making up the reproduction function, the creation of the initial population and termination criteria and the evaluation function are required. Implementation of the genetic algorithm is according to the following procedure:

Coding

Variables should be coded in chromosome structures in order to use genetic algorithm. Chromosome representation includes a binary encoding using either zeros or ones or binary alphabet.

Fitness function

A fitness function based on the objective function should be constructed in order to create the optimization process and the process of next generation selection. The fitness function measures the goodness of a solution to evaluate and rank chromosomes in a population. Chromosomes with a high fitness value have more chance to be chosen as parents in comparison with lower fitness value. A fitness function is derived from the objective function which can be described as Eq. (8) [14].

$$F(x) = \frac{1}{1 + f(x)} \tag{8}$$

Where $F(x)$ is fitness function and $f(x)$ is objective function.

Basic operation of the algorithm

Main operators of the algorithms are reproduction, crossover and mutation.

Reproduction

This is the first operator of the algorithm which copies individual strings into a separate string according to their fitness values. It is called mating pool.

Crossover

The crossover is the second genetic operator which is mostly responsible for the progress of the search. The operator exchanges some part of two or more chromosomes to reproduce new offspring with the hope of collecting all good features of previous ones.

Mutation

Mutation is applied after crossover to provide a small randomness into the new chromosome. The aim is to keep diversity in the population in order to get a quicker convergence.

VIRTUAL MACHINING FOR MONOTORING AND MINIMIZING THE TOOL DEFLECTION ERROR

In order to implement the proposed method, a software is developed in the research work to monitor and minimize the tool deflection errors. The theoretical tool path (NC codes) are generated by a CAD/CAM system. Having the cutting tool geometry and machining parameters as input to the software, every tool deflection error is calculated at each cutter path. Finally, the errors are applied to the G-Codes and the corresponding modified NC codes according to actual machining path are developed.

Optimization strategies

The first objective function of the software is minimizing the tool deflection error. In order to minimize the error, cutting forces of Eq. (7) should be minimized. According to the Eq. (3) and Eq. (4), feed rate as well as spindle speed have direct effect on the cutting forces of Eq. (7).

Minimizing the machining time is also an objective function which should be considered to utilize the machine more effectively. Machining time for milling operation can be described as Eq. (9) [30].

$$t_m = \frac{K}{f} \tag{9}$$

Where K and f are the distance to be traveled by tool to perform the operation (mm) and feed rate (mm/min) respectively.

Maximizing tool life is another objective function of the software. It is affected by various parameters such as cutting speed, feed rate, depth of cut, chip thickness, tool geometry and cutting fluid. Tool life can be shown as Eq. (10) [30].

$$T_L = \left(\frac{60}{Q}\right)\left[\frac{C\left(\frac{G}{5}\right)^g}{V(A)^w}\right]^{\frac{1}{m}} \tag{10}$$

Where Q is the contact proportion of cutting edge with workpiece per revolution, C is 33.98 for the HSS tools and 100.05 for the carbide tools , $g = 0.14$, V is cutting speed (mm/minutes) , $w = 0.28$, m is 0.15 for HSS tools while it reaches a maximum of 0.30 for carbide tools, G and A are slenderness ratio and chip cross-section which can be shown as Eq. (11) and Eq. (12) respectively [30].

$$G = \frac{a}{f} \tag{11}$$

$$A = a.f \tag{12}$$

Where a and f are axial depth of cut (mm) and feed rate (mm/minutes) respectively.

Surface roughness is also another objective function which should be minimized. The arithmetic value of surface roughness in end milling can be shown as Eq. (13) [30].

$$R_a = 318\frac{f^2}{4d} \tag{13}$$

Where f and d are feed rate (mm/minutes) and cutter diameter (mm) respectively.

The surface roughness presented in Eq. (13) is under influence of feed rate and cutter diameter. By decreasing the feed rate the surface roughness will be improved. But, a suitable feed rate should be selected with regard to the other objective functions such as machining time as well as tool life. Also, increasing spindle speed can reduce the cutting forces in Eq. (7). But, tool life is a challenge for efficiency of part production. As a result, all the parameters should be optimized in order to achieve the most appropriate results.

An algorithm which can optimize the machining parameters using genetic algorithm is considered in the presented software. The method is based on minimizing

Journal of Manufacturing Science and Engineering. Received September 08, 2015;
Accepted manuscript posted December 31, 2015. doi:10.1115/1.4032393

unnecessary cutting forces, machining times, surface roughness and maximizing tool life. The input to the system is the geometry of cutting tool, measured cutting forces, desired amount of population size, chromosome length, probability of crossover and probability of mutation. Next, variables are coded in chromosome structures with binary encoding using either zeros or ones. Fitness functions based on the objective functions of cutting forces, machining time, tool life and surface roughness are constructed to be used in evolution of population generated by chromosomes. So, chromosomes in the population are evaluated and ranked by using the fitness functions in order to select the chromosomes with higher fitness values. The operator of crossover is used to reproduce new offspring by exchanging some part of two or more chromosomes. In order to provide a quicker convergence, mutation is applied after crossover. The results are compared to the most appropriate outputs of objective functions with regard to the acceptable range of machining parameters. If better results can be achieved, they are saved. Else, the population of chromosomes is evaluated again by using the fitness functions in order to create the most appropriate output. As a result, optimized machining parameters such as feed rate and spindle speed are introduced.

Flowchart and strategy of machining parameters optimization by genetic algorithm is presented in Fig. 4.

The algorithm of the optimization method is presented in appendix B.

Software and algorithm verification

Visual Basic programming language is used for the development of the software. The initial input to the software are the theoretical machining G-Codes of the part, cutting tool parameters and cutting forces. The output of the software are the actual machining G-Codes which can produce the part with regard to tool deflection errors. The algorithms of the software is presented in appendix C.

To calculate the tool deflection error, the cutting forces of the milling operation should be calculated. As a result, a dialogue box for calculating the cutting forces according to machining parameters and tool details is presented. The software considers four models of tools due to different cutting edge angles to calculate the cutting forces. Fig. 5 shows the dialogue box of cutting forces.

Another dialogue box is provided as shown in Fig. 6 to provide the ability of monitoring the tool deflection error along tool path.

Fig. 7 shows the dialog box of machining parameters optimizer.

The actual G-Codes according to the tool deflection error of real machined parts are generated with a text format file in order to be used by the CAM softwares such as Vericut [31].

Vericut is a 3D solid-based CAM software that interactively simulates the material removal process of an NC program [31]. The program depicts multi-axis milling/drilling , multi-axis turning and combination of mill/turn machining operations in order to verify the accuracy as well as quality of an NC program [31].

VALIDATION

In order to experimentally validate the virtual machining software, a spline curve as a free form profile is considered for machining and comparison in real and virtual environments. Tool deflection errors of real and virtual machined parts with optimized machining parameters are also compared with other parts in order to present the ability of the error minimization.

The CNC machine tool used for the present study is a 3-axis EMCO VMC600. The workpiece material is AL7075T6 and the cutting tool used is 10 mm diameter HSS flat end mill, helix angel 30° and flute number 4. The spline profile has 0.33 mm radial and 10 mm axial depth of cut. Cutting force model of Engin and Altintas [22] is used. In order to estimate the cutting coefficients, the average cutting forces of twenty slot milling tests with 1.5 mm axial depth of cut were measured by Kistler dynamometer. By increasing the feed rate, the average of cutting forces increase linearly which shows a coherent relation between them. For fitting the experimental cutting forces with respect to feed rate, linear curve fitting is used and the diagram is obtained as shown in Fig. 8.

The cutting force coefficients are as Eq. 15.

$$\begin{aligned} &K_{tc} = 937.334, K_{te} = 5.0386 \\ &K_{rc} = 292.067, K_{re} = 6.7597 \\ &K_{ac} = 171.37, K_{ae} = -0.83067 \end{aligned} \tag{15}$$

After supplying the error measurement data and G-Codes into the software, the error enforced G-Codes are generated. The cutting tests were carried out on the same three-axis machine tool in Vericut environment by generated G-Codes after tool deflection error enforcement. After machining in Vericut, machined parts were inspected for contour errors at some designated key points by CAD surface comparator

Journal of Manufacturing Science and Engineering. Received September 08, 2015;
Accepted manuscript posted December 31, 2015. doi:10.1115/1.4032393

software in order to find the errors of part in virtual environment. Fig. 9 shows the profile of the test workpiece.

Machining G-Codes of part without errors are as Fig. 10.

Where spindle speed and feed rate are 1000 rpm and 100 mm/minutes respectively. The developed software enforces tool deflection error by error model of Eq. (1). The new G-Codes are as Fig. 11.

The workpiece is measured by ZEISS CMM machine in order to find error distances of nominal and machined profile. Distances between machined and nominal profiles of real part are shown in Fig. 12.

Distances between each point of virtual machined part and nominal profile are shown in Fig. 13.

The optimization is applied by the software on the machining parameters with a population size of 25, iterated for 200 generations and crossover and mutation probability are selected to be 0.9 and 0.001, respectively. As a result, the spindle speed and feed rate are calculated as 1232 rpm and 82 mm/min respectively.

Distances between each point of real machined part with optimized machining parameters and nominal profile are shown in Fig. 14. As a result, a reduction in tool deflection errors of real machined parts shown in Fig. 12 and Fig. 14 are achieved by using optimized machining parameters.

Distances between each point of virtual machined part with optimized machining parameters and nominal profile are shown in Fig. 15. So, tool deflection errors of virtual machined parts shown in Fig. 13 and Fig. 15 are decreased as a result of deploying optimized machining parameters.

A comparison for predicted cutting forces without and with optimization for five selected points along the profile of machined parts is presented in Fig. 16. Optimized machining parameters have decreased the cutting forces as shown in Fig. 16.

Profile errors along the curve length are as Fig. 17.

Where real part 1 and real part 2 are parts without and with optimized machining parameters respectively. Also, virtual part 1 and virtual part 2 are parts in virtual environment without and with optimized machining parameters respectively.

CONCLUSION

In the present work, the tool deflection errors are enforced on G-Codes of parts in order to produce actual parts with free form surfaces in virtual environment. Optimization technique based on genetic algorithm is used to determine the optimized machining parameters in order to minimize the tool deflection error. Visual Basic programming language is used to develop the virtual machining software. As a result, an effective methodology in the virtual environment is provided to monitor and minimize the error.

Having the cutting tool information and machining codes of a part, the amount of tool deflection errors are estimated by calculating the cutting forces. A new part is then produced in virtual environment with regard to the tool deflection error of actual machined part. Furthermore, optimized parameters of machining based on genetic algorithms are obtained to minimize the tool deflection error.

Journal of Manufacturing Science and Engineering. Received September 08, 2015;
Accepted manuscript posted December 31, 2015. doi:10.1115/1.4032393

A free form spline is machined by using the developed procedure. An 86.4 % compatibility is obtained in comparison between real and virtual machined parts. Using optimized parameters of machining, real and virtual machined parts are also produced. An 88.2 % compatibility is obtained in comparison between real and virtual machined parts with optimized machining parameters.

Using optimized machining parameters, 23.3 % and 23.6% reduction in tool deflection error are obtained for real and virtual machined parts respectively.

In order to calculate and compare the surface roughness of virtual parts machined without and with optimized machining parameters a CAD software is used. A 47.1 % and 48.8% reduction in surface roughness (R_a) are obtained for real and virtual machined parts respectively. Also the time of machining increased from 65.4 sec. to 79.8 sec.

The optimized parameters obtained by the genetic algorithm also improve the accuracy and quality of the produced part by reducing the tool deflection error. The system can be developed further to a 5-axis CNC milling machine in order to generate and monitor the error of more sophisticated parts in the virtual environment. This is the concept of future research of the authors.

APPENDIX A

$$h(\varphi_j, k) = S_{tj} Sin(\varphi_j) Sin(k_j) \tag{A.1}$$

Where S_{tj} , ϕ_j and κ_j are feed per tooth, radial lag angle and axial immersion angle of tooth j respectively.

$$\begin{cases} dF_x(\varphi_j) = -dF_t \cos\varphi_j - dF_r \sin\varphi_j \\ dF_y(\varphi_j) = +dF_t \sin\varphi_j - dF_r \cos\varphi_j \\ dF_z(\varphi_j) = +dF_a \end{cases} \tag{A.2}$$

APPENDIX B

10 Encode genes of the process parameters by binary encoding

20 Determine fitness functions

30 Generate initial population

40 Evaluate the population by fitness functions

50 Exchange some part of two chromosomes to generate new offspring by crossover

60 Apply mutation on the population

70 Evaluate each individual or chromosome by constrains

80 If result is acceptable then go to 110

90 Else

100 Go to 40

110 End if

120 Consider optimized machining parameters

130 END

APPENDIX C

1- Input

Read file: G-Code of parts with text format (*.Text)

Show text file in text box1

Split (text1) for elements recognition (G01, G02, G03, X, Y, Z, R…)

2-Error Enforcement

Journal of Manufacturing Science and Engineering. Received September 08, 2015;
Accepted manuscript posted December 31, 2015. doi:10.1115/1.4032393

2-1- tool deflection error

Open force calculator dialog

Read machining parameters (Feed rate, Depth of cut, Spindle Speed) from G-Codes file

Select kind of cutting tool (Flat end, Ball nose end, Ball end, Taper end) by user

Import cutting tool details (Lengths, Number of flutes, Diameters) by user

Select material of workpiece for cutting force coefficient (Ktc,Krc,Kac,Kte,Kre,Kae)

Calculate cutting forces as Fx, Fy, Fz for different rotation angels of tool cutting edge between entering and existing angles

Show the cutting force results in text box

Calculate average of cutting force of each position for finding tool deflection error

Close force calculation dialog

Open tool deflection error dialog

Calculate amount of tool deflection errors by calculated cutting force of each position

Show tool deflection error results in the monitoring dialog

Add amount of tool deflection errors to G-Codes

Close tool deflection dialog

3- Minimizing tool deflection error

Open tool deflection error dialog

Open dialog of machining parameters optimization

Find optimized machining parameters according to the algorithm of appendix C

Show results of optimized machining parameters in the dialog of machining parameters optimization

Close dialog of machining parameters optimization

Calculate amount of tool deflection errors according to the optimized machining parameters

Close tool deflection error dialog

4- Write file

Join (text1)

Show in text2

5- Output

Save as new G-Codes with Text format (*.Text)

FUNDING

Fund of the research is provided by Department of Mechanical Engineering, Amirkabir University of Technology (Tehran Polytechnic).

REFERENCES

[1] Lo´ pez de Lacalle, L. N., Lamikiz, A., Sa´ nchez, J. A., and Salgado, M. A., 2007, "Toolpath selection based on the minimum deflection cutting forces in the programming of complex surfaces milling," Int. J. Mach. Tools Manuf., **47**(2), pp. 388–400.

[2] Rao, V. S., and Rao, P. V. M., 2006, "Tool deflection compensation in peripheral milling of curved geometries," Int. J. Mach. Tools Manuf., **46**(15), pp. 2036–2043.

[3] Ryu, S. H., 2012, "An analytical expression for end milling forces and tool deflection using Fourier series," Int. J. Adv. Manuf. Technol., **59**(1-4), pp. 37–46.

[4] Dow, T. A., Miller, E. L., and Garrard, K., 2004, "Tool force and deflection compensation for small milling tools," Precis. Eng., **28**(1), pp. 31–45.

[5] Smaoui, M., Bouaziz, Z., Zghal, A., Dessein, G., and Baili, M., 2011, "Simulation of the deflected cutting tool trajectory in complex surface milling," Int. J. Adv. Manuf. Technol., **56**(5-8), pp. 463–474.

[6] Ong, T. S., and Hinds, B. K., 2003, "The application of tool deflection knowledge in process planning to meet geometric tolerances," Int. J. Mach. Tools Manuf., **43**(7), pp. 731–737.

[7] Zeroudi, N., and Fontaine, M., "Prediction of tool deflection and tool path compensation in ball-end milling," J. Intell. Manuf. DOI 10.1007/s10845-013-0800-8.

[8] Kivanc, E. B., and Budak, E., 2004, "Structural modeling of end mills for form error and stability analysis," Int. J. Mach. Tools Manuf., **44**(11), pp. 1151–1161.

[9] Nojedeh, M. V., Habibi, M., and Arezoo, B., 2011, "Tool path accuracy enhancement through geometrical error compensation," Int. J. Mach. Tools Manuf., **51**(6), pp. 471–482.

[10] Eskandari, S., Arezoo, B., and Abdullah, A., 2013, "Positional, geometrical, and thermal errors compensation by tool path modification using three methods of regression, neural networks, and fuzzy logic," Int. J. Adv. Manuf. Technol., **65**(9-12), pp. 1635-1649.

[11] Habibi, M., Arezoo, B., and Nojedeh, M. V., 2011, "Tool deflection and geometrical error compensation by tool path modification," Int. J. Mach. Tools Manuf., **51**(6), pp. 439–449.

[12] Soori, M., Arezoo, B., and Habibi, M., 2013, "Dimensional and geometrical errors of three-axis CNC milling machines in a virtual machining system," Comput. Aided Des., **45**(11), pp. 1306-1313.

[13] Soori, M., Arezoo, B., and Habibi, M., 2014, "Virtual machining considering dimensional, geometrical and tool deflection errors in three-axis CNC milling machines," J. Manuf. Syst., **33**(4), pp. 498-507.

[14] Palanisamy, P., Rajendran, I., and Shanmugasundaram, S., 2007, "Optimization of machining parameters using genetic algorithm and experimental validation for end-milling operations," Int. J. Adv. Manuf. Technol., **32**(7-8), pp. 644–655.

[15] Cus, F., Milfelner, M., and Balic, J., 2006, "An intelligent system for monitoring and optimization of ball-end milling process," J. Mater. Process Technol., **175**(1), pp. 90–97.

[16] Milfelner, M., Cus, F., and Balic, J., 2005, "An overview of data acquisition system for cutting force measuring and optimization in milling," J. Mater. Process Technol., **164**, pp. 1281–1288.

[17] Kumar, A. S., Adam Khan, M., Thiraviam, R., and Sornakumar, T., 2006, "Machining parameters optimization for alumina based ceramic cutting tools using genetic algorithm," Machine. Sci. Technol., **10**, pp. 471-489.

[18] D'Addona, D. M., and Teti, R., 2013, " Genetic algorithm-based optimization of cutting parameters in turning processes," Procedia CIRP., **7**, pp. 323–328.

[19] Jameel, A., Minhat, M., and Nizam, Md., 2013, " Using genetic algorithm to optimize machining parameters in turning operation: a review," Int. J. Sci. Res. Pub., **3**, pp. 1–6.

[20] Merdol, S. D., and Altintas, Y., 2008, " Virtual cutting and optimization of three-axis milling processes," Int. J. Mach. Tools Manuf., **48**(10), pp. 1063-1071.

[21] Kivanc, E. B., and Budak, E., 2004, "Structural modeling of end mills for form error and stability analysis," Int. J. Mach. Tools Manuf., **44**(11), pp. 1151-1161.

[22] Engin, S., and Altintas, Y., 2001, "Mechanics and dynamics of general milling cutters.: Part I: helical end mills," Int. J. Mach. Tools Manuf., **41**(15), pp. 2195-2212.

[23] Erdim, H., Lazoglu, I., and Ozturk, B., 2006, "Feed rate scheduling strategies for free form surfaces," Int. J. Mach. Tools Manuf., **46**(7), pp. 747-757.

[24] Salami, R., Sadeghi, M. H., and Motakef, B., 2007, "Feed rate optimization for 3-axis ball end milling of sculptured surfaces," Int. J. Mach. Tools Manuf., **47**(5), pp. 760-767.

Journal of Manufacturing Science and Engineering. Received September 08, 2015;
Accepted manuscript posted December 31, 2015. doi:10.1115/1.4032393

[25] Guzel, B. U., and Lazoglu, I., 2004, "Increasing productivity in sculptured surface machining via off-line piecewise variable feed rate scheduling based on the force system model," Int. J. Mach. Tools Manuf., **44**(1), pp. 21-28.

[26] Fu, H. J., Devor, R. E., and Kapoor, S. G., 1984, "A mechanistic model for the prediction of the force system in face milling operation," ASME J. Eng. Ind., **106**(1), pp. 81–88.

[27] Yucesan, G., and Altıntaş, Y., 1996, "Prediction of ball end milling forces," ASME, J. Eng. Ind., **118**(1), pp. 95-103.

[28] Budak, E., and Tekeli, A., 2005, "Maximizing chatter free material removal rate in milling through optimal selection of axial and radial depth of cut pairs," Ann. CIRP, **54**(1), pp. 353-356.

[29] Altintas, Y., and Merdol, S. D., 2007, "Virtual high performance milling," Ann. CIRP, **56**(1), pp. 81-84.

[30] Rad, M. T., Bidhendi, I. M., 1997, "On the optimization of machining parameters for milling operations," Int. J. Mach. Tools Manuf., **37**(1), pp. 1-16.

[31] About VERICUT Software, accessed 26 August 2015, <http://www.cgtech.com/products/about-vericut/>.

Journal of Manufacturing Science and Engineering. Received September 08, 2015;
Accepted manuscript posted December 31, 2015. doi:10.1115/1.4032393

Figure Captions List

Journal of Manufacturing Science and Engineering. Received September 08, 2015;
Accepted manuscript posted December 31, 2015. doi:10.1115/1.4032393

Fig. 16 Comparison of predicted cutting forces without and with optimization for five selected points along the profile of machined parts

Fig. 17 Profile errors along the curve length

Fig. 1

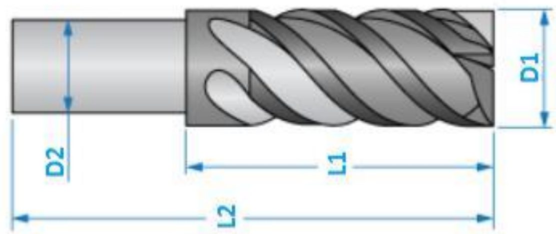

Fig. 2

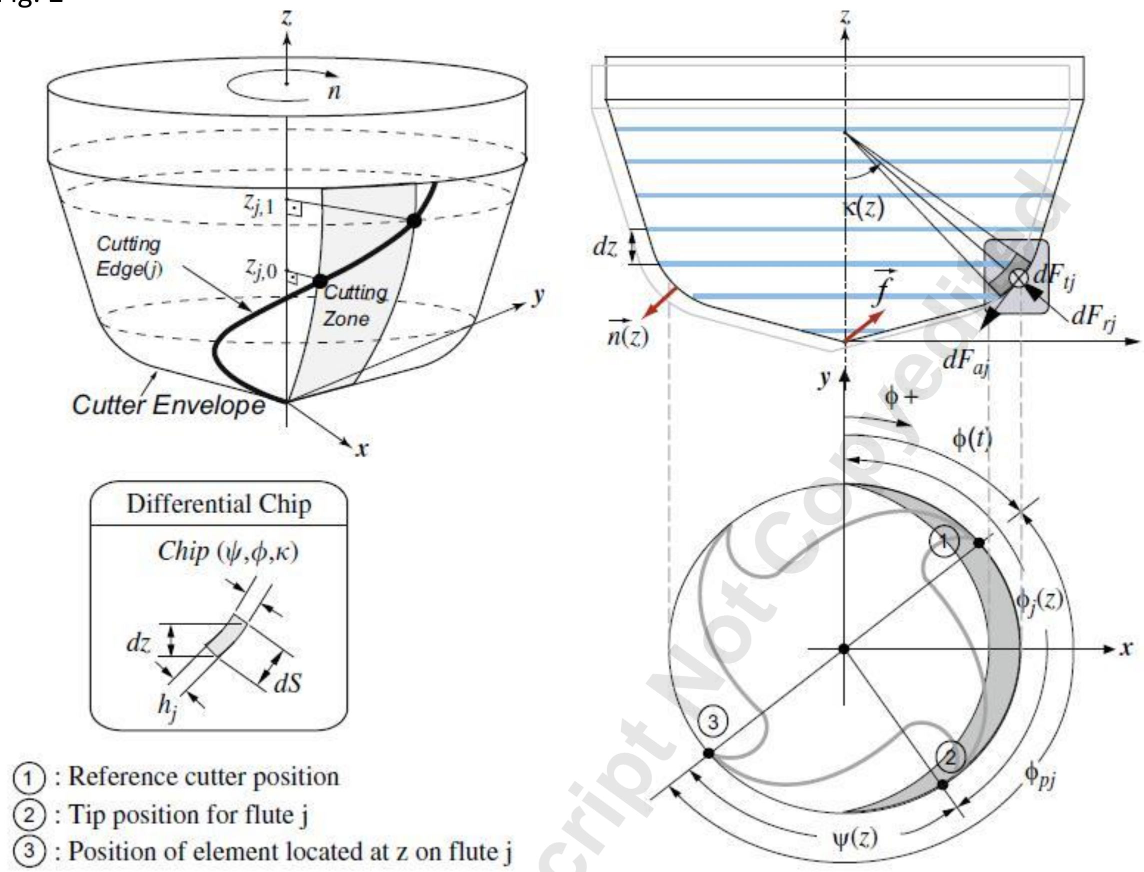
z
n
$z_{j,1}$
Cutting Edge(j)
$z_{j,0}$
Cutting Zone
y
Cutter Envelope
x
Differential Chip
Chip (ψ,ϕ,κ)
dz
dS
h_j
1 : Reference cutter position
2 : Tip position for flute j
3 : Position of element located at z on flute j
z
$\kappa(z)$
dz
dF_{tj}
$\vec{f}$
$\vec{n}(z)$
dF_{rj}
dF_{aj}
y
$\phi +$
$\phi(t)$
$\phi_j(z)$
x
ϕ_{pj}
$\psi(z)$

Fig. 3

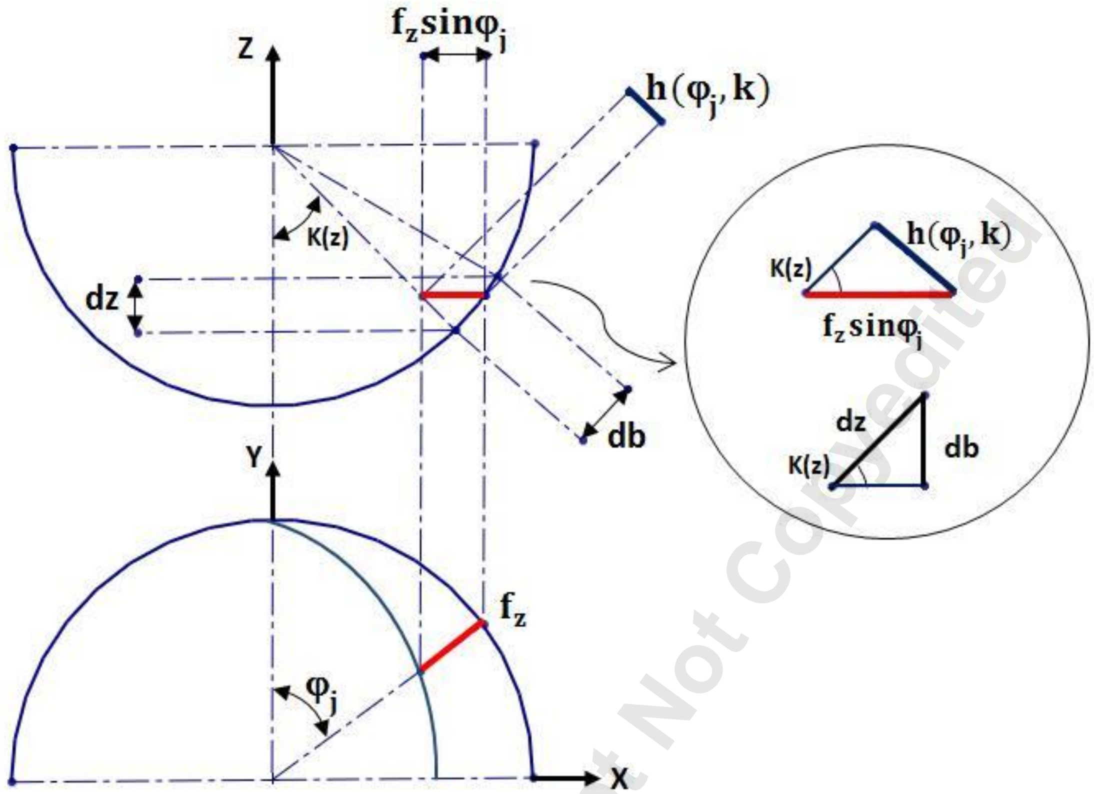
$f_z \sin\varphi_j$
Z
$h(\varphi_j, k)$
K(z)
dz
db
Y
f_z
φ_j
X
K(z)
$h(\varphi_j, k)$
$f_z \sin\varphi_j$
dz
K(z)
db

Journal of Manufacturing Science and Engineering. Received September 08, 2015;
Accepted manuscript posted December 31, 2015. doi:10.1115/1.4032393

Fig. 4

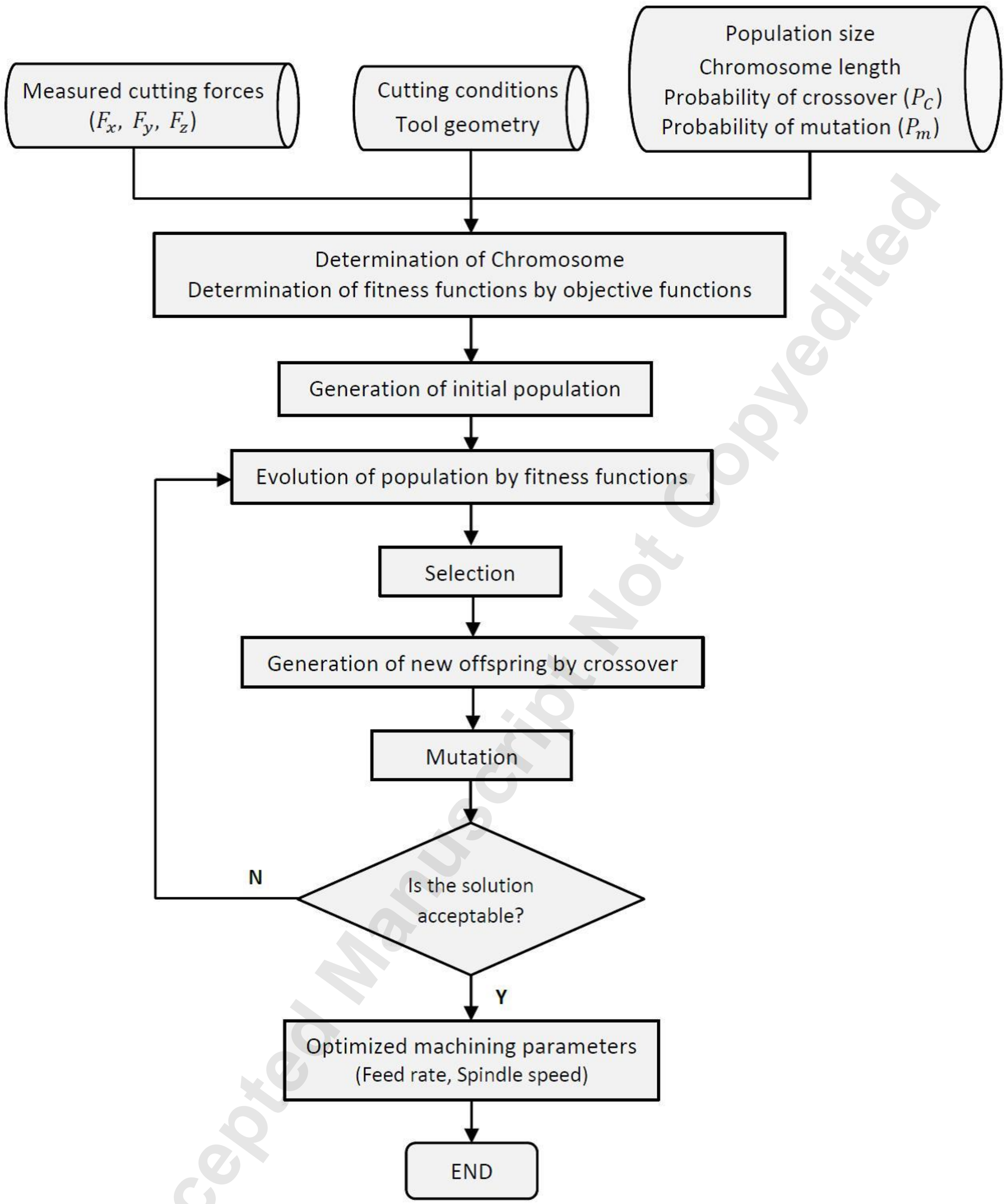

Journal of Manufacturing Science and Engineering. Received September 08, 2015;
Accepted manuscript posted December 31, 2015. doi:10.1115/1.4032393

Fig. 5

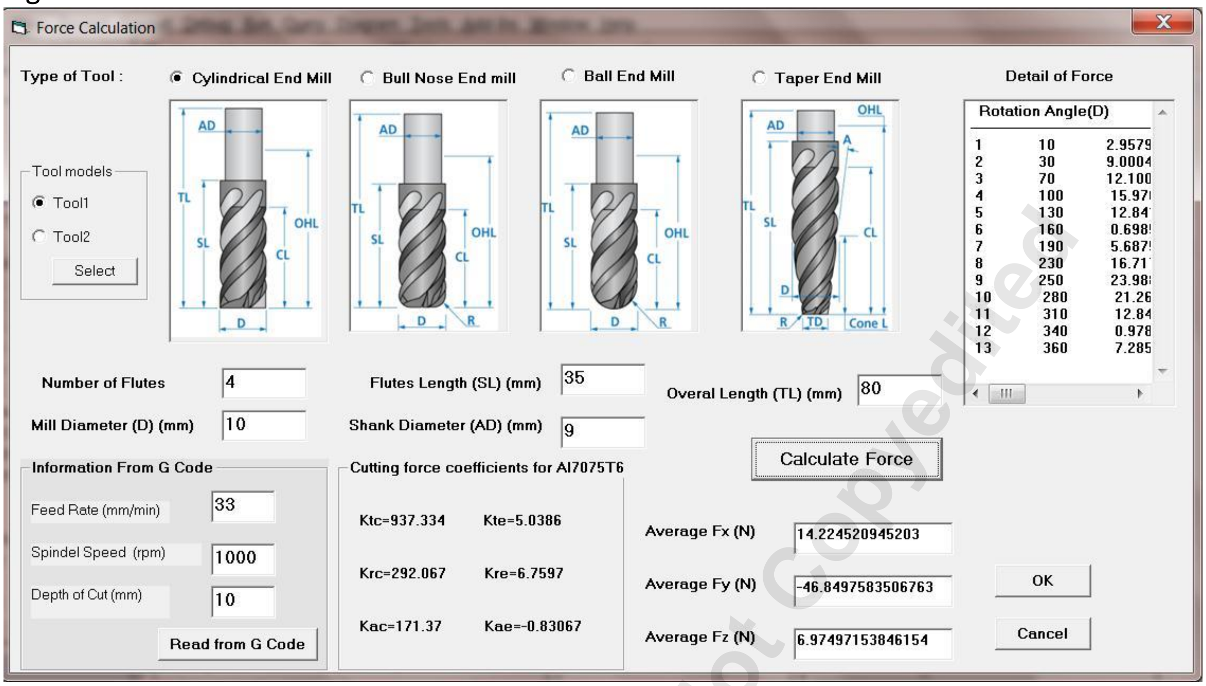

Fig. 6

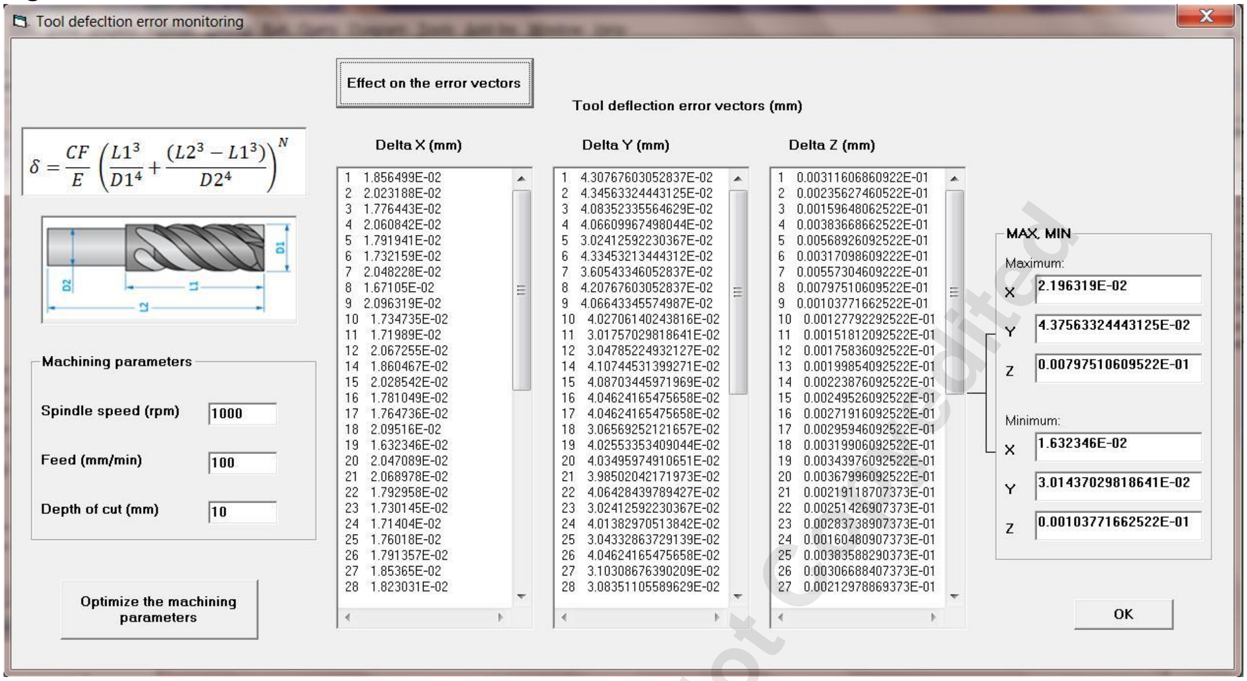
Tool defecltion error monitoring
Effect on the error vectors
Tool deflection error vectors (mm)
$\delta = \frac{CF}{E}\left(\frac{L1^3}{D1^4} + \frac{(L2^3 - L1^3)}{D2^4}\right)^N$
D1
D2
L1
L2
Machining parameters
Spindle speed (rpm) 1000
Feed (mm/min) 100
Depth of cut (mm) 10
Optimize the machining parameters
Delta X (mm)
1 1.856499E-02
2 2.023188E-02
3 1.776443E-02
4 2.060842E-02
5 1.791941E-02
6 1.732159E-02
7 2.048228E-02
8 1.67105E-02
9 2.096319E-02
10 1.734735E-02
11 1.71989E-02
12 2.067255E-02
14 1.860467E-02
15 2.028542E-02
16 1.781049E-02
17 1.764736E-02
18 2.09516E-02
19 1.632346E-02
20 2.047089E-02
21 2.068978E-02
22 1.792958E-02
23 1.730145E-02
24 1.71404E-02
25 1.76018E-02
26 1.791357E-02
27 1.85365E-02
28 1.823031E-02
Delta Y (mm)
1 4.30767603052837E-02
2 4.34563324443125E-02
3 4.08352335564629E-02
4 4.06609967498044E-02
5 3.02412592230367E-02
6 4.33453213444312E-02
7 3.60543346052837E-02
8 4.20767603052837E-02
9 4.06643345574987E-02
10 4.02706140243816E-02
11 3.01757029818641E-02
12 3.04785224932127E-02
14 4.10744531399271E-02
15 4.08703445971969E-02
16 4.04624165475658E-02
17 4.04624165475658E-02
18 3.06569252121657E-02
19 4.02553353409044E-02
20 4.03495974910651E-02
21 3.98502042171973E-02
22 4.06428439789427E-02
23 3.02412592230367E-02
24 4.01382970513842E-02
25 3.04332863729139E-02
26 4.04624165475658E-02
27 3.10308676390209E-02
28 3.08351105589629E-02
Delta Z (mm)
1 0.00311606860922E-01
2 0.00235627460522E-01
3 0.00159648062522E-01
4 0.00383668662522E-01
5 0.00568926092522E-01
6 0.00317098609222E-01
7 0.00557304609222E-01
8 0.00797510609522E-01
9 0.00103771662522E-01
10 0.00127792292522E-01
11 0.00151812092522E-01
12 0.00175836092522E-01
13 0.00199854092522E-01
14 0.00223876092522E-01
15 0.00249526092522E-01
16 0.00271916092522E-01
17 0.00295946092522E-01
18 0.00319906092522E-01
19 0.00343976092522E-01
20 0.00367996092522E-01
21 0.00219118707373E-01
22 0.00251426907373E-01
23 0.00283738907373E-01
24 0.00160480907373E-01
25 0.00383588290373E-01
26 0.00306688407373E-01
27 0.00212978869373E-01
MAX, MIN
Maximum:
X 2.196319E-02
Y 4.37563324443125E-02
Z 0.00797510609522E-01
Minimum:
X 1.632346E-02
Y 3.01437029818641E-02
Z 0.00103771662522E-01
OK

Journal of Manufacturing Science and Engineering. Received September 08, 2015;
Accepted manuscript posted December 31, 2015. doi:10.1115/1.4032393

Fig. 7

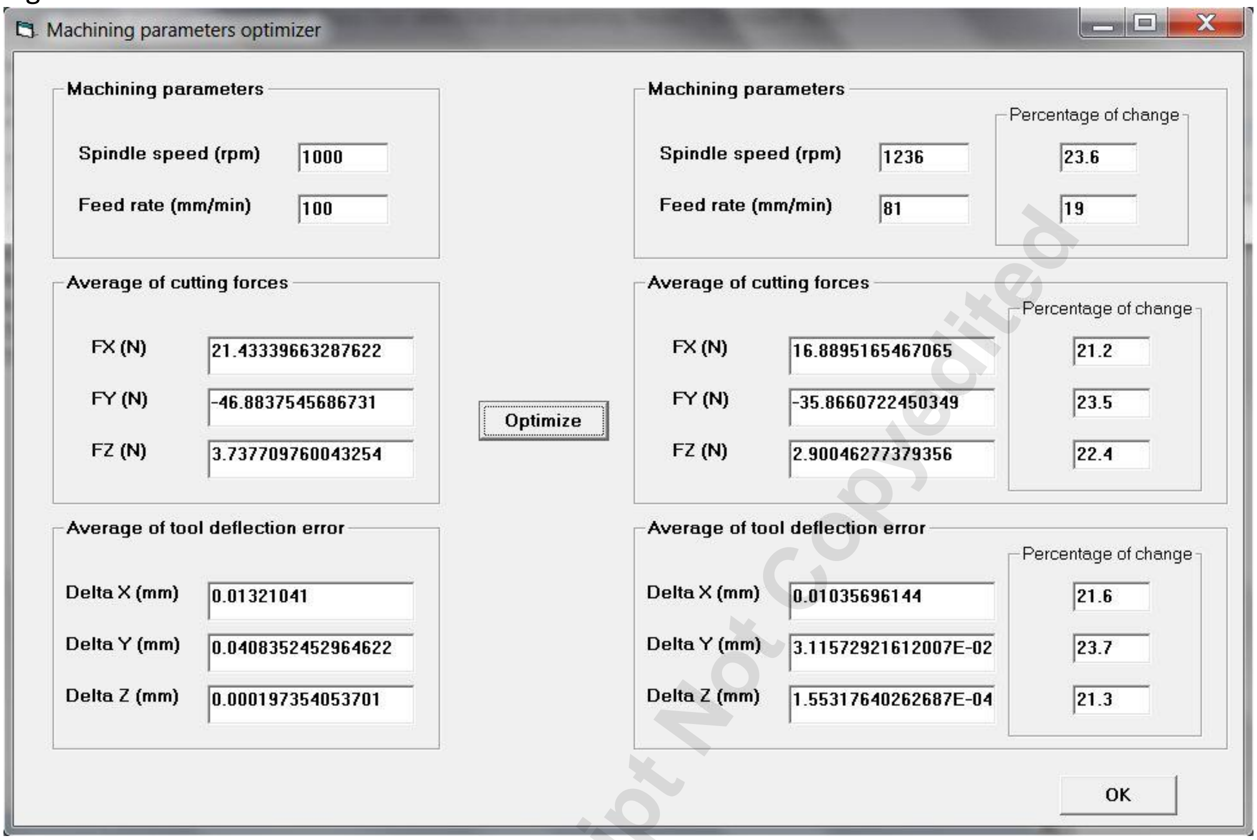

Journal of Manufacturing Science and Engineering. Received September 08, 2015;
Accepted manuscript posted December 31, 2015. doi:10.1115/1.4032393

Fig. 8

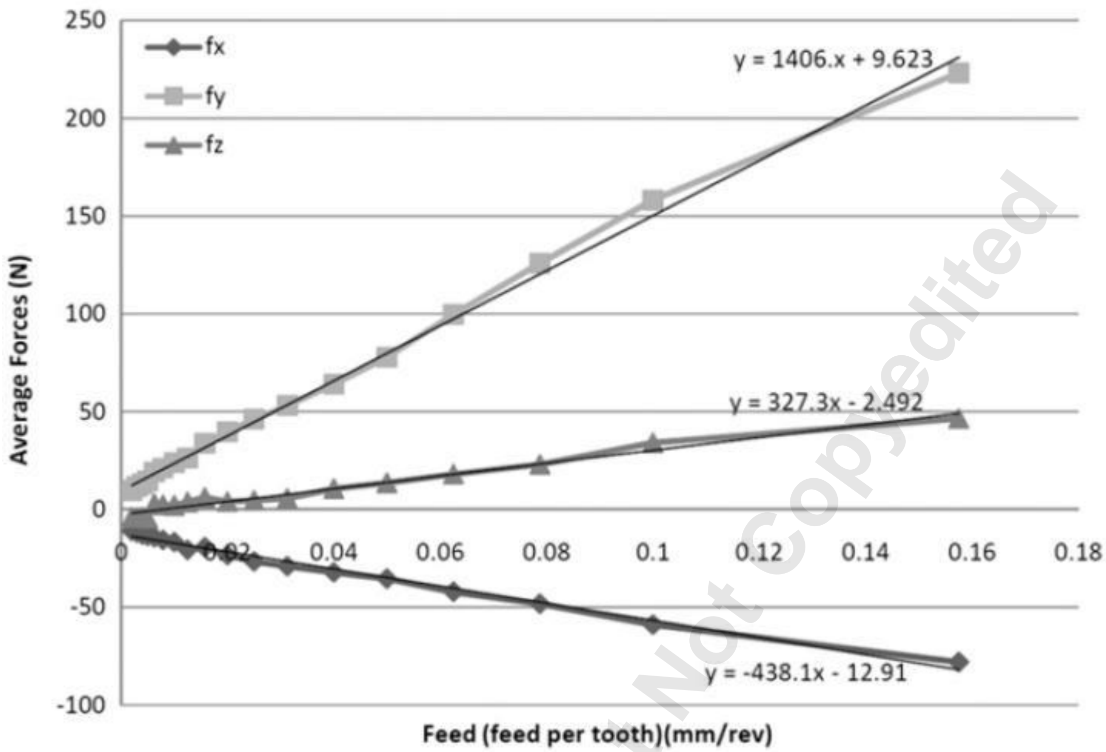

Journal of Manufacturing Science and Engineering. Received September 08, 2015;
Accepted manuscript posted December 31, 2015. doi:10.1115/1.4032393

Fig. 9

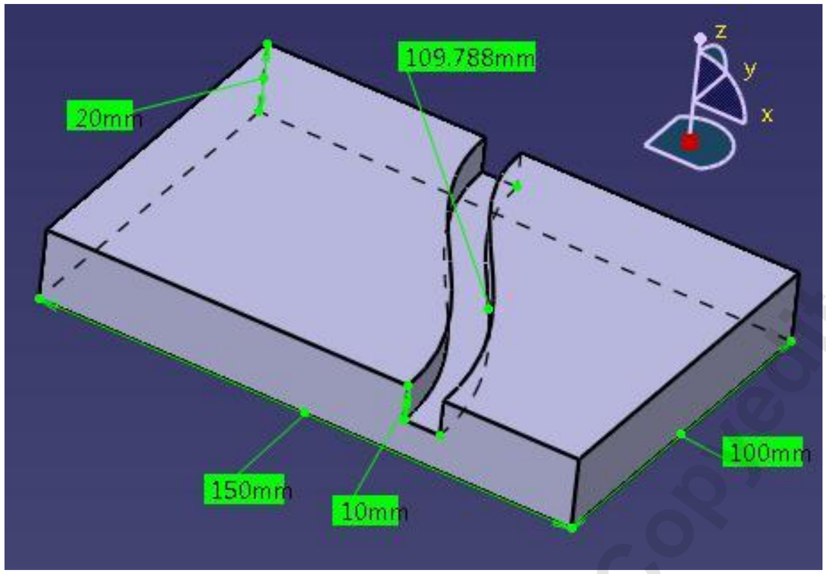

Journal of Manufacturing Science and Engineering. Received September 08, 2015;
Accepted manuscript posted December 31, 2015. doi:10.1115/1.4032393

Fig. 10

File Edit Format View Help

```
%
O5000 (F_CONTOUR  _T1_2.TAP)
( MCV-OP ) (11-JUL-2012)
(SUBR  OUTINES: O2 .. O0)
G90 G17
G80 G49 G40
G54
G91 G28 Z0
G90
M01
N1 M6 T1
(TOOL -1- MILL DIA 10.0 R  0. MM )
G90 G00 G40 G54
G43 H1 D31 G0 X 104.81 Y -0.007 Z50. S1000 M3
M8
(-----------------------)
(F-CONTOUR  -T1-2 - PR  OFILE)
(-----------------------)
G0 X 104.81 Y -0.007 Z10.
G0 Z2.
G1 Z -10. F 33
G3 X 104.152 Y 8.706 R 58.823 F100
G3 X 101.975 Y 17.794 R 55.944
G3 X 99.681 Y 23.741 R 62.09
G3 X 96.85 Y 29.474 R 76.985
G3 X 94.054 Y 34.304 R 102.884
G3 X 91.119 Y 38.907 R 153.613
G3 X 87.544 Y 44.185 R 295.404
G1 X 83.037 Y 50.698
G2 X 79.212 Y 56.4 R 275.894
G2 X 75.718 Y 62.023 R 157.641
G2 X 72.286 Y 68.307 R 107.127
G2 X 69.531 Y 74.406 R 83.864
G2 X 66.9 Y 82.197 R 71.611
G2 X 64.615 Y 96.613 R 66.563
G2 X 64.53 Y 99.993 R 70.661
G0 Z10.
M30
```

Journal of Manufacturing Science and Engineering. Received September 08, 2015;
Accepted manuscript posted December 31, 2015. doi:10.1115/1.4032393

Fig. 11

```
%
O5000 (F_CONTOUR 1_T1.TAP)
( MCV-OP ) (26-JUN-2012)
(SUBR OUTINES: O2 .. O0)
G90 G17
G80 G49 G40
G54
G91 G28 Z0
G90
M01
N1 M6 T2
(TOOL -1- MILL DIA 10.0 R 0. MM )
G90 G00 G40 G54
G43 H1 D31 G0 x 104.7788 y -0.01012 Z50. S1000 M3
M8
(----------------------)
(F-CONTOUR-T2 - PROFILE)
(----------------------)
G0 x 104.7788 y -0.01012 Z10.
G0 Z2.
G1 z -10. F 33
G3 x  103.4528  y 8.6909  R  58.8231
G3 x  101.4628  y 17.7029 R  55.8238
G3 x  99.6499   y 23.7379 R  62.0900
G3 x  96.8189   y 29.4709 R  76.9850
G3 x  94.0229   y 34.3009 R  102.8840
G3 x  91.0879   y 38.9039 R  153.6130
G3 x  87.5174   y 44.1819 R  295.4040
G1 x  83.0104   y 50.6950
G2 x  79.1854   y 56.3970 R  275.8939
G2 x  75.6914   y 62.0198 R  157.6410
G2 x  72.2594   y 68.3038 R  107.1270
G2 x  69.5004   y 74.4028 R  83.8640
G2 x  66.8694   y 82.1938 R  71.6110
G2 x  64.5845   y 96.6098 R  66.5630
G2 x  64.4995   y 99.9898 R  70.6610
G0 Z10.
```

Journal of Manufacturing Science and Engineering. Received September 08, 2015;
Accepted manuscript posted December 31, 2015. doi:10.1115/1.4032393

Fig. 12

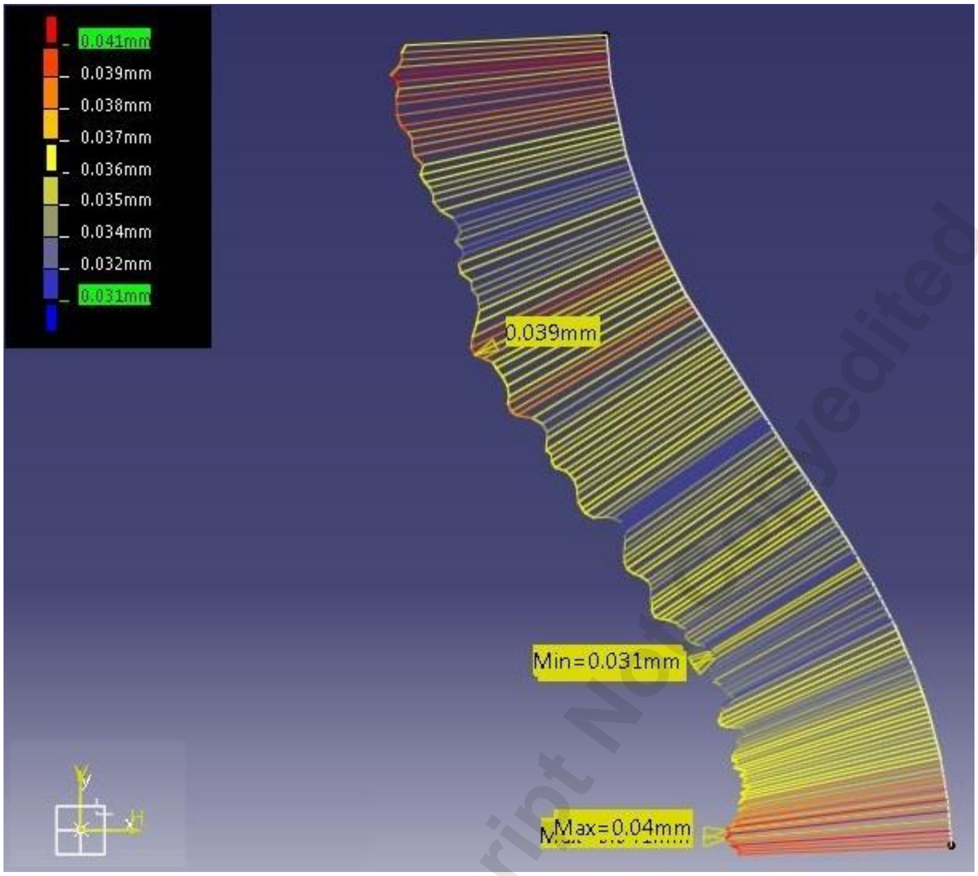

Fig. 13

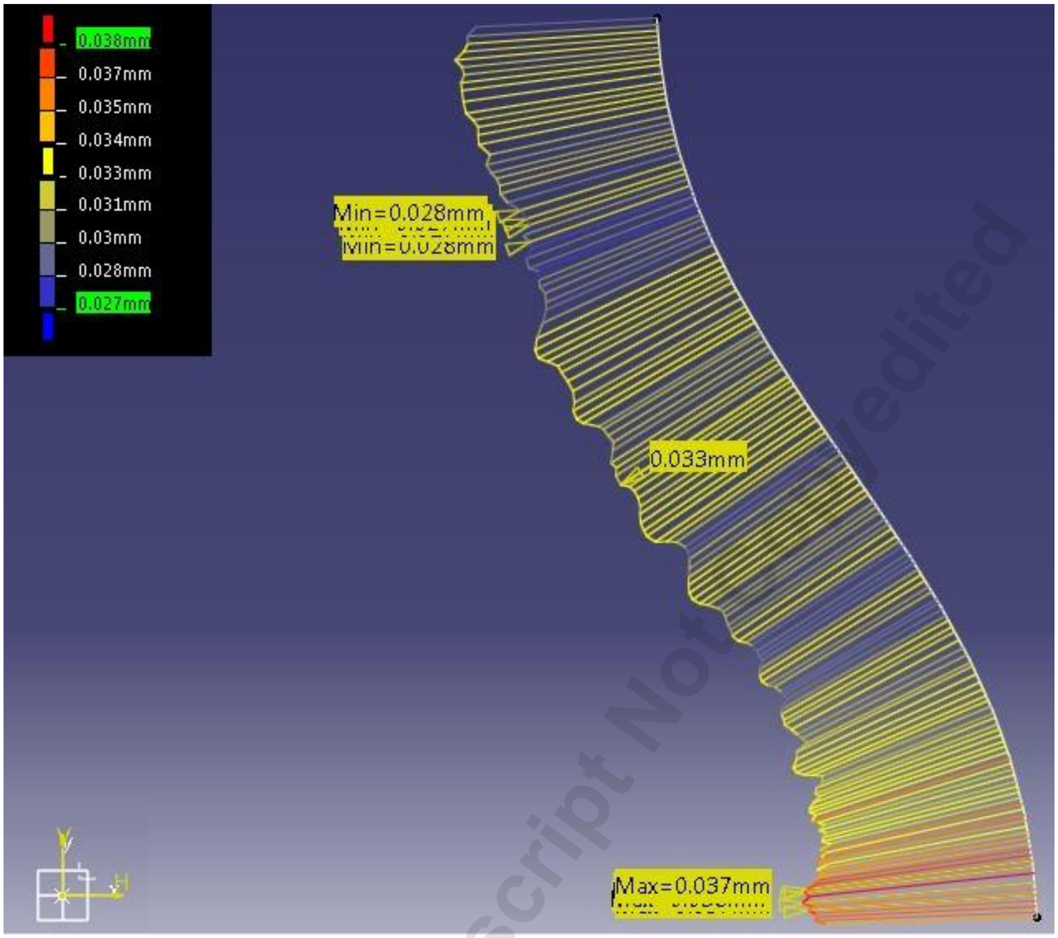
0.038mm
0.037mm
0.035mm
0.034mm
0.033mm
0.031mm
0.03mm
0.028mm
0.027mm
Min=0.028mm
0.033mm
Max=0.037mm

Journal of Manufacturing Science and Engineering. Received September 08, 2015;
Accepted manuscript posted December 31, 2015. doi:10.1115/1.4032393

Fig. 14

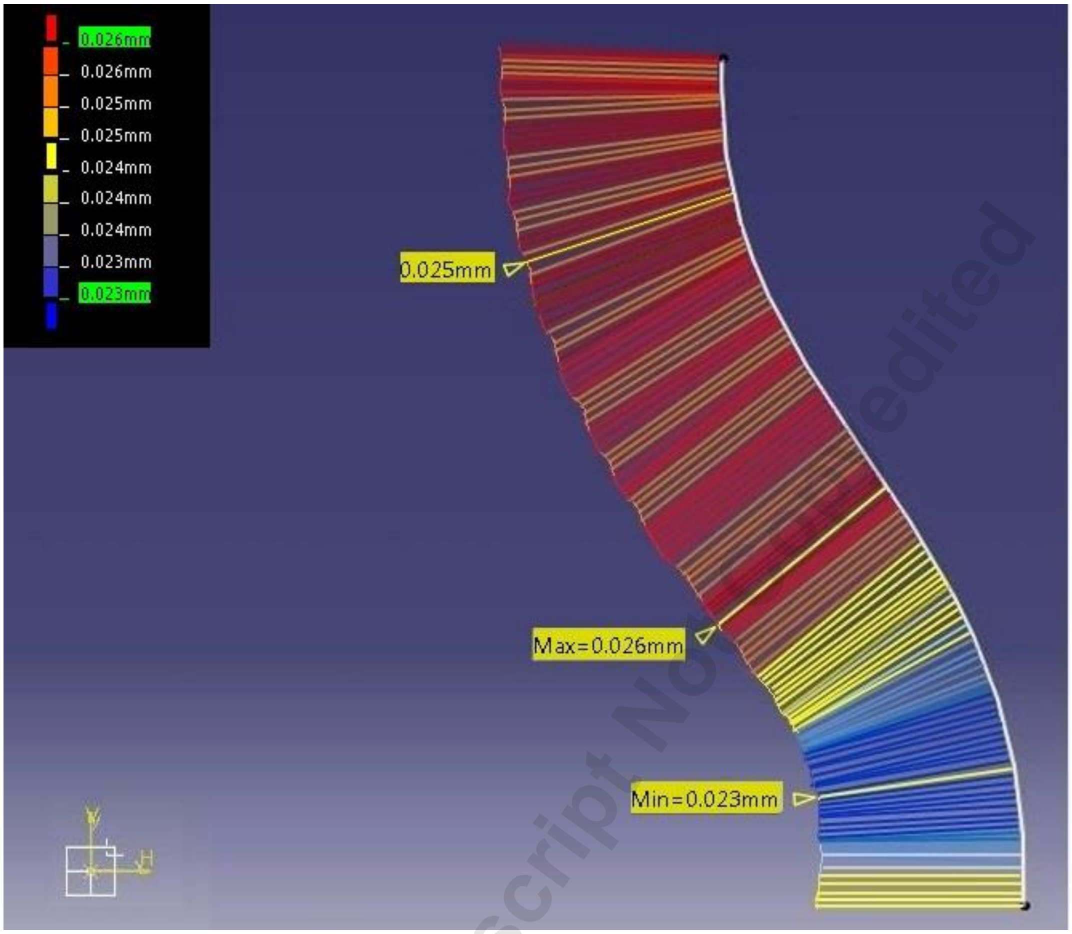

Journal of Manufacturing Science and Engineering. Received September 08, 2015;
Accepted manuscript posted December 31, 2015. doi:10.1115/1.4032393

Fig. 15

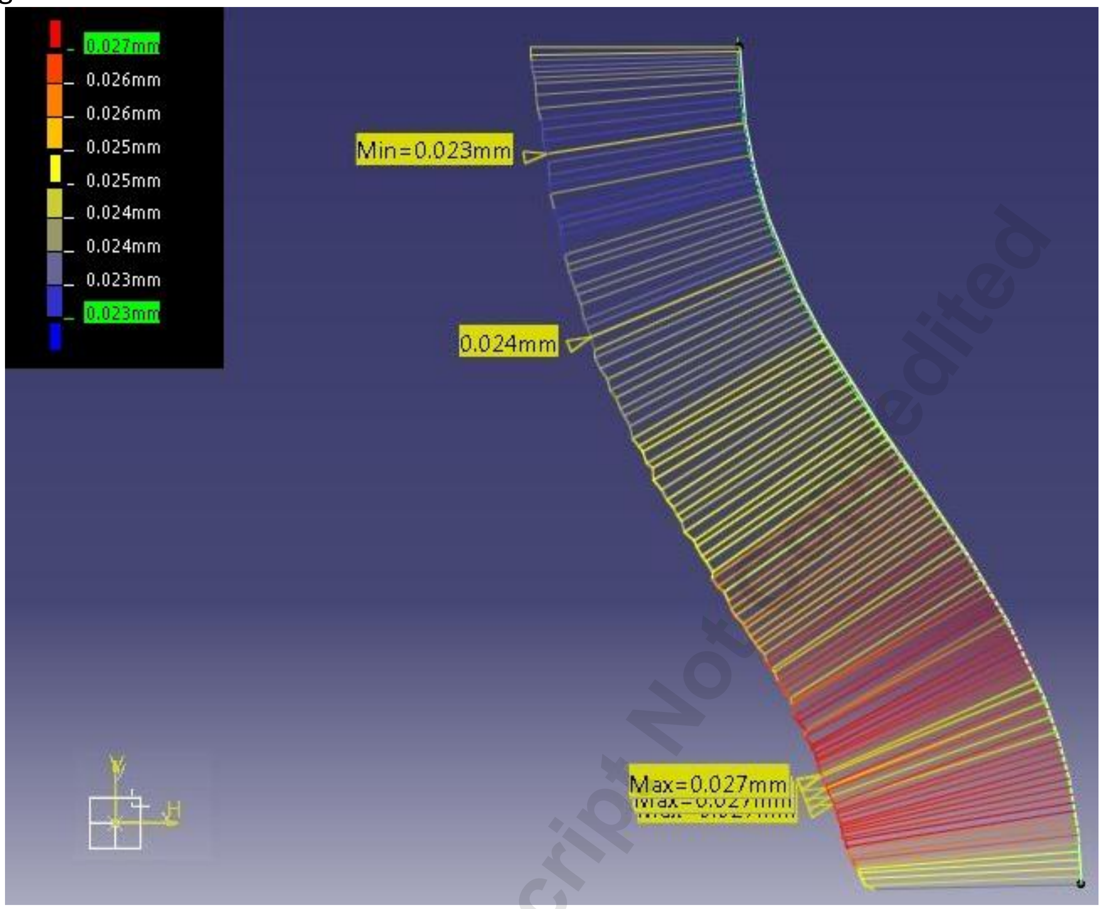

Journal of Manufacturing Science and Engineering. Received September 08, 2015;
Accepted manuscript posted December 31, 2015. doi:10.1115/1.4032393

Fig. 16

		Before optimization	After optimization	Percentage of change
Point 1	FX(N)	22.45667746	17.44883839	22.3
	FY(N)	-45.74665949	-34.40148794	24.8
	FZ(N)	3.953228109	3.0518921	22.8
Point 2	FX(N)	23.87644032	18.48036481	22.6
	FY(N)	-44.85440606	-33.68565895	24.9
	FZ(N)	3.80644674	2.896705969	23.9
Point 3	FX(N)	24.40513631	19.18243714	21.4
	FY(N)	-44.08062345	-32.75190322	25.7
	FZ(N)	3.651031107	2.760179517	24.4
Point 4	FX(N)	23.976233022	18.62953306	22.3
	FY(N)	-43.53005319	-32.77813005	24.7
	FZ(N)	3.359885002	2.536713177	24.5
Point 5	FX(N)	25.40766535	19.46227166	23.4
	FY(N)	-44.63957602	-33.97071735	23.9
	FZ(N)	3.583126039	2.77692268	22.5

Journal of Manufacturing Science and Engineering. Received September 08, 2015;
Accepted manuscript posted December 31, 2015. doi:10.1115/1.4032393

Fig. 17